IOPscience iopscience.iop.org

Home Search Collections Journals About Contact us My IOPscience

Global phase diagrams for charge transport in two dimensions

This article has been downloaded from IOPscience. Please scroll down to see the full text article.

1993 J. Phys. A: Math. Gen. 26 L811

(http://iopscience.iop.org/0305-4470/26/17/011)

View the table of contents for this issue, or go to the journal homepage for more

Download details:
IP Address: 171.66.16.68
The article was downloaded on 01/06/2010 at 19:29

Please note that terms and conditions apply.

J. Phys. A: Math. Gen. 26 (1993) L811–L817. Printed in the UK

LETTER TO THE EDITOR

Global phase diagrams for charge transport in two dimensions

C A Lütken†

Department of Physics, University of Oxford, 1 Keble Road, Oxford OX1 3NP, UK

Received 19 April 1993

Abstract. It is suggested that it is not necessary to solve the full non-perturbative problem of two-dimensional charge transport in order to obtain global information about the phase and flow diagrams for the quantum Hall system and its relatives. It is argued that the effective quantum field theories encoding the macroscopic properties of these systems are invariant under a symmetry contained in the modular group. New phase and flow diagrams are obtained which exhibit a hierarchy of only odd or only even phases (Hall plateaus). The Kramers–Wannier-like symmetry determines the exact location of all renormalization group fixed points, which appear to be in agreement with available scaling experiments on the quantum Hall system. It also explains the observed 'super-universality', of the delocalization exponent.

Partition functions may be invariant under two different types of transformations: symmetries of the action (or Hamiltonian) and symmetries of the parameter space. We are perhaps most familiar with the former, which include spacetime invariances as well as gauge symmetries. It is the purpose of this letter to focus on the latter and show how such symmetries can be used to elicit global information about the phase diagram and renormalization group (RG) flow of the system.

The motivation for these considerations comes from an attempt [1] to understand the 'macroscopic' properties of the subtle and resilient quantum Hall system. The main result is a new phase and RG-flow diagram for this system, which unlike the one proposed earlier [1] can only be valid in the strong magnetic field limit, where even denominator plateaus are forbidden. In spite of the great difference between these diagrams, it will be clear from the group-theoretical considerations below that they are closely related. The global phase and flow diagrams presented here encode various aspects of electron transport in two dimensions, and may account for all the peculiar universality properties which have been observed in this system.

Transport coefficients or response functions are macroscopic quantities appearing in the effective action, which encodes only the low energy properties of the system. At large scales they parametrize the space on which the renormalization group acts, and it is the phase and fixed point structure of this parameter (conductivity or resistivity) space which is explored when resistances are measured. Since these are global properties of the effective field theory, it would appear that a theoretical determination of these data is a hopeless non-perturbative task. However, in [1] a way around this impasse was suggested. The main idea is that the observation of only a single

† Present address: NORDITA, Blegdamsvej 17, DK-2100 Copenhagen Ø, Denmark.

0305-4470/93/170811+07 $07.50 © 1993 IOP Publishing Ltd

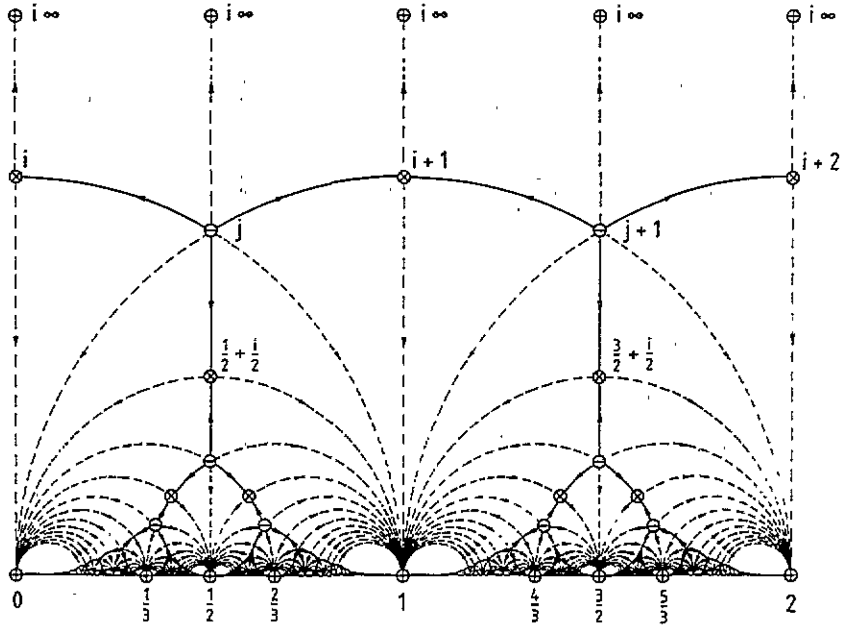

Figure 1. Phase and flow diagram associated with the modular group Γ(1), showing both 'odd' and 'even' phases.

scaling exponent for all available transitions indicates the existence of an infinite global discrete parameter space symmetry, analogous to the Kramers–Wannier (KW) duality [2] exhibited by most spin systems. This may be sufficient to determine the geometry of the phase and RG-flow diagram, including the exact location of all renormalization group fixed points. Using only the most rudimentary experimental data as input, it is surprisingly easy to make a 'phenomenological ansatz' for the form of this symmetry.

It appears to be very difficult to *prove* that such a symmetry follows from the microphysics [3], but because it leads to a wealth of experimentally accessible predictions. such an ansatz is far from vacuous. Indeed, not only does it correlate all scaling data and suggest new experiments, because the symmetries we have in mind are not easily satisfied they should also be very useful for pinning down the correct effective quantum field theory [3].

In the following we shall study two-parameter flows constrained by subgroups of the modular group $\Gamma(1)\equiv SL(2,\mathbb{Z})$. These groups act on the complex upper half plane $\mathbb{H}=\{\sigma\in\mathbb{C}|Im\,\sigma>0\}$. The modular group is generated by any two non-commuting fractional linear transformations acting on $\mathbb{H}$. It is convenient and conventional to choose $T\colon\sigma\to\sigma+1$ and $S\colon\sigma\to-1/\sigma$.

Consider first the main group-theoretical facts [4, 5] determining the tree-like structure of the modular invariant phase diagram shown in figure 1, which first appeared in the context of coupled clock models [6]. The modular group is the free product of $\mathbb{Z}_2(S)$ and $\mathbb{Z}_3(TS)$. This implies that there are two types of 'elliptic' fixed points on the tree, of order two ($S^2=1$) and three ($(TS)^3=1$), which are located at i and $j\equiv\exp(\pi i/3)$, respectively, and at images of these points under the group. The fixed points of order two are natural candidates for delocalization fixed points (⊗), and this also fits well with scaling data on the transition between many integer levels

[1]. In addition, there are two other types of fixed points not located on the self-dual tree. Strictly speaking, they do not lie in the parameter space $\mathbb{H}$ at all, but on its compactification $\bar{\mathbb{H}} = \mathbb{H} \cup \mathbb{Q} \cup \{i\infty\}$. The rationals $\mathbb{Q}$ are 'parabolic' fixed points of $\Gamma(1)$, and are to be identified with the attractive RG fixed points ($\oplus$ in figure 1) corresponding to Hall plateaus. The 'hyperbolic' fixed point at $i\infty$, which is also an attractor in this case, seems to be associated with some kind of metallic or superconducting phase.

From the fact that the phases of the diagram in figure 1 only touch the real axis at fractional values, it is immediately clear why $\Gamma(1)$ is a promising group for the quantum Hall problem: if σ can be identified with the *complexified conductivity* $\sigma = \sigma_{xy} + i\sigma_{xx}$, then σ_{xy} will be forced by the phase-diagram alone to take fractional values when σ_{xx} vanishes. Note that in this effective field theoretical description no distinction is made between integer and fractional phases, and we cannot have one without the other.

It is the purpose of this letter to explore the properties of phase and flow diagrams associated with subgroups of $\Gamma(1)$. One of the motivations for this is that the phase and flow diagram invariant under the full modular group shown in figure 1 contains both 'even' and 'odd' phases, while the experiments *predominantly* turn up only 'odd' phases. A phase is uniquely characterized by the value of the conductivity at the attractive fixed point to which it is attached (i.e. for which it is the basin of attraction or universality class): $\sigma_{\oplus} = \sigma_{xy} = p/q \in \mathbb{Q}$. If the denominator q is odd (even) the phase is called odd (even). Since experiments are turning up even fractions at an increasing rate it is encouraging that they are not disallowed by the family of infinite discrete symmetries that we are considering. On the other hand, we should be able to 'switch them off' in a very strong magnetic field (B), since in this case the electron spins are completely polarized so that the spin degree of freedom is frozen out. This means that the spatial part of the many-body wave-function must be completely anti-symmetric, and consequently, by a standard argument due to Laughlin [7], only odd phases can appear in such a system. We shall see that this is exactly what happens if the $B \to \infty$ limit breaks $\Gamma(1)$ to a subgroup $\Gamma_T(2)$, to be discussed next.

Since we want to retain only half the phases, but still cover the conductivity plane, we should look for a smaller group than $\Gamma(1)$. Consider therefore the congruence subgroups of $\Gamma(1)$ at level two [4]. These all lie between $\Gamma(1)$ and $\Gamma(2)$, where

$$\Gamma(N) \equiv \{\gamma \in SL(2, \mathbb{Z}) | \gamma = I \,(\mathrm{mod}\, N)] \qquad (1)$$

is called the principal congruence group at level N. Obviously $\Gamma(1) = SL(2, \mathbb{Z})$. A congruence group is a group that contains $\Gamma(N)$ for some finite value of N. At level two there are only four congruence groups in addition to $\Gamma(2)$. The three of interest to us are defined as follows:

$$\Gamma_R(2) \equiv \{\gamma \in \Gamma(1) | \gamma = I, R (\mathrm{mod}\, 2)\} \qquad (2)$$

where $R = T, S, W\ (W = TST)$. Each of these groups is generated by two non-commuting generators, which we can choose as follows:

$$\Gamma_T(2) = \{T, ST^2S\} \qquad \Gamma_S(2) = \{S, T^2\} \qquad \Gamma_W(2) = \{W, T^2\}. \qquad (3)$$

To see what these symmetries have to do with the quantum Hall system, note that we are interested in symmetries which partition the rationals into the various equivalence classes which appear in the quantum Hall experiments. Clearly $\Gamma(1)$ maps any rational number into any other, which is why every rational number labels one of the phases in the $\Gamma(1)$-invariant phase diagram (figure 1). There are, however, other ways to tesselate the upper half plane, which is reflected in the way $\Gamma \subset \Gamma(1)$ treats the rationals.

The special significance of the principal congruence group $\Gamma(2)$ is that it respects the parity of the fraction $p/q \in \mathbb{Q}$, i.e. if p is even (odd) then so is its image under $\gamma \in \Gamma(2)$, and similarly for q. Thus $\Gamma(2)$ splits the rationals into three equivalence classes, which, if we let '0' denote 'even' and '1' denote 'odd', are conveniently labelled by $0/1=0$, $1/1=1$ and $1/0=\infty$. (0/0 is ill-defined, i.e. there is no 0/0 class because two even numbers are not relatively prime.) The congruence groups $\Gamma_T(2)$, $\Gamma_S(2)$ and $\Gamma_W(2)$, being intermediate between $\Gamma(1)$ and $\Gamma(2)$, splits the rationals into just two equivalence classes each: because $\Gamma_T(2)$ contains T it maps 0 to 1, because $\Gamma_S(2)$ contains S it maps 0 to ∞, and because $\Gamma_W(2)$ contains W it maps 1 to ∞. In short, these groups partition the rationals $p/q \in \mathbb{Q}$ as follows:

$$
\begin{aligned}
&\Gamma(1): && \{0\sim 1\sim\infty\}=\mathbb{Q}\\
&\Gamma_T(2): && \{0\sim 1,\ \infty\}=\{q\in 2\mathbb{Z}+1\}\cup\{q\in 2\mathbb{Z}\}\\
&\Gamma_S(2): && \{0\sim\infty,\ 1\}=\{pq\in 2\mathbb{Z}\}\cup\{pq\in 2\mathbb{Z}+1\}\\
&\Gamma_W(2): && \{0,\ 1\sim\infty\}=\{p\in 2\mathbb{Z}+1\}\cup\{p\in 2\mathbb{Z}+1\}\\
&\Gamma(2): && \{0,1,\ \infty\}=\mathbb{Q}_{0/1}\cup\mathbb{Q}_{1/1}\cup\mathbb{Q}_{1/0}.
\end{aligned}
\tag{4}
$$

This result makes it clear that it is $\Gamma_T(2)$ which is of interest in the quantum Hall problem. It is the main proposition of this letter that the effective theory of the spin-polarized quantum Hall system is $\Gamma_T(2)$-invariant.

Notice that $\Gamma_T(2)$ is the group implicitly assumed in the so-called 'hierarchy generating mechanism' [7–9], which was invented in order to account for the observed fractions (see also [10]). To see this recall that if a ground state with 'filling factor' ν appears, then the particle-hole conjugate state with filling factor $1-\nu$, as well as the quasi-particle condensate with filling factor $\nu/(2\nu+1)$ should also be ground states of the quantum Hall system. Since ν is essentially the Hall conductivity on the plateaus, we see that these are fractional linear transformations on σ restricted to act only on the real axis. The first transformation is $TJ=JT$, where J: $\sigma \to -\bar{\sigma}$ is a so-called 'outer automorphism' of $\Gamma(1)$. J is in fact the only automorphism of $\Gamma(1)$ not in $\Gamma(1)$, and since J is rather trivial we will continue to suppress it here. The other transformation is the inverse of ST^2S, which together with T generates $\Gamma_T(2)$, according to (3).

Having identified the subgroup of the modular group of interest in the quantum Hall problem, we now wish to know how the phase and flow diagram is modified. Since the elliptic fixed points of $\Gamma(1)$ of order three (the bifurcation points) are not fixed points of any of its subgroups, only the full modular group will give rise to a tree-shaped phase diagram (figure 1). Furthermore some, *but not all*, elliptic fixed points of order two also disappear when subgroups are considered. So we still have both attractive fixed points, at the odd fractions, say, as well as saddle points $\otimes$. There must then also be repulsive fixed points, and they can no longer be the bifurcation points. *The only remaining candidates are the even parabolic fixed points, which are the ones* we set out to eliminate from the spectrum of attractors anyway. This leads to the phase and flow diagram in figure 2.

The easiest way to construct the phase and flow diagrams associated with other groups is to study the RG potentials for the flows. This gives a geometrical verification of the diagrams in figures 1 and 2, and generates distinct hierarchies that may be of interest for 'relatives' of the quantum Hall system [11], including the frustrated Heisenberg antiferromagnet and high-temperature superconductivity. Lee and Fisher [12], for example, construct a 'bosonic' hierarchy of anyon superconducting states, which appears to be generated by $\Gamma_S(2)$. Due to space limitations these ideas must be discussed elsewhere [13].

We should now ask whether the new diagram in figure 2 is contradicted by the scaling experiments reported in [14] and [15]. Clearly the surprising 'super-universality' of delocalization fixed points (⊗), which was the original motivation for considering KW-like symmetries [1], is still maintained: the surviving elliptic fixed points of order two have not moved and are still related by symmetries. Only data for integer delocalization transitions are available so far, and they appear to coincide with the values

$$\sigma^{E_2}_{\mathrm{int}} = \left(n + \frac{1}{2}\right) + \frac{i}{2} \qquad (n = 0, 1, 2, \ldots) \tag{5}$$

predicted by modular invariance.

However, the absence of bifurcation points from figure 2 means that the data reported in [15] on the location of so-called 'mobility fixed points' must be reinterpreted. The experiments in [15] tried to locate the largest value of σ_{xx} associated with the fractional phases $p/q = k/(2k+1)$ $(k = 1, 2, 3, 4, (5))$. In [1] it was suggested that these be identified with the points at which the $\Gamma(1)$-tree bifurcates to give room for the new phases. The imaginary parts of these points, which appear at

$$\sigma^{E_3} = \frac{4k^2 - 2k + 3}{2(4k^2+3)} + \frac{\sqrt{3}i}{2(4k^2+3)} \tag{6}$$

are surprisingly close to the observed values $\sigma_{xx}^{\mathrm{MFP}}$ reported in [15], see table 1.

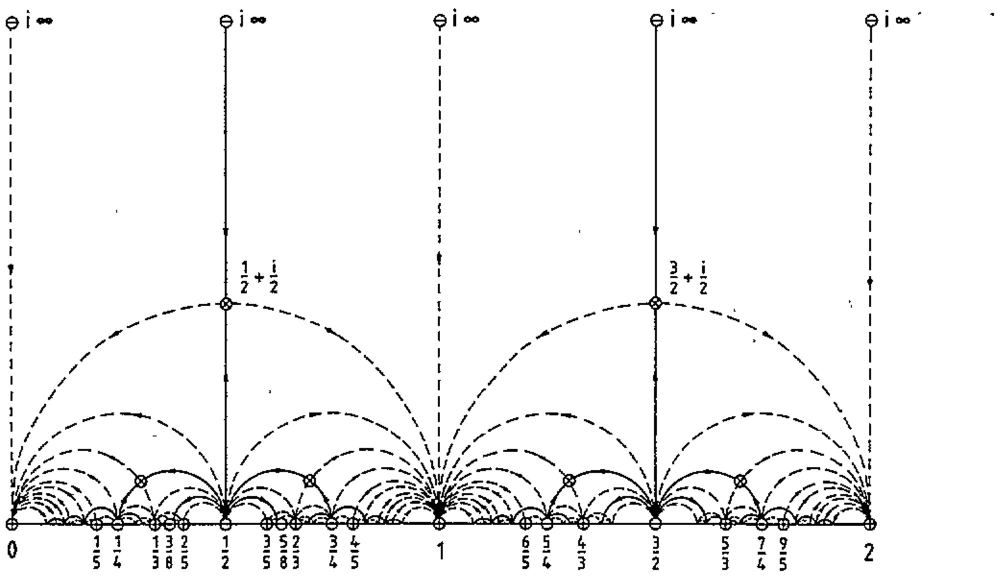

Figure 2. Phase and flow diagram associated with the subgroup $\Gamma_T(2)$ of the modular group, showing only 'odd' phases.

Table 1. Experimental data σ_{xx}^{MFP} on the location of mobility fixed points, obtained in [15] by studying temperature driven flows in the σ-plane, compared with the imaginary part σ_{xx}^{*} of various points associated with the appearance of new phases in the $\Gamma(1)$-invariant (figure 1) and $\Gamma_T(2)$-invariant (figure 2) flow diagrams. The errors are estimated in [16].

$k/(2k+1)$	σ_{xx}^{MFP}	$\sigma_{xx}^{E_2}$	$\sigma_{xx}^{E_3}$	σ_{xx}^{max}
1/3	0.15 ± 0.03	0.1000	0.1237	0.1250
2/5	0.055 ± 0.01	0.0294	0.0456	0.0625
3/7	0.025 ± 0.005	0.0135	0.0221	0.0417
4/9	0.013 ± 0.003	0.0077	0.0129	0.0313
5/11	$0.01\pm?$	0.0050	0.0084	0.0250

The $\Gamma_T(2)$-invariant 'bush' shown in figure 2 clearly does not admit such an interpretation. Instead, it seems natural to compare the data with the dissipative conductivity at the 'apex' of these phases, which is given by $\sigma_{xx}^{max}=1/8k$. Since this 'bush' is an offspring of the modular invariant 'tree', these points cannot be very far removed from the bifurcation points. Indeed, we see from table 1 that it is hard to distinguish between $\sigma_{xx}^{E_3}$ and σ_{xx}^{max} for small k, for which the data presumably are also most reliable. For larger values of k $\sigma_{xx}^{E_3}$ appears to be in better agreement with the data, but in view of the large uncertainties in these experiments† σ_{xx}^{max} also cannot be ruled out.

For completeness, and comparison with future experiments, table 1 also contains the corresponding information about the location of the delocalization fixed points associated with these fractional phases:

$$\sigma^{E_2}=\frac{4k^2-2k+1}{2(4k^2+1)}+\frac{i}{2(4k^2+1)}. \tag{7}$$

These points are $\Gamma_T(2)$-images of the integer delocalization point $1/2+i/2$, and are most easily located by using the algorithm described in [1]. It is clear that better experiments are needed in order to map out the phase diagram and fixed point structure of the quantum Hall system.

After this work was completed two preprints appeared where conclusions which seem to be similar to those reported here and in [1] have been reached in a different way. Halperin *et al* [17] display a phase diagram which is topologically similar to figure 1, while Kivelson *et al* [18] have found a phase diagram in the resistivity plane ($\rho=\rho_{xy}+i\rho_{xx}$) which appears to be similar to figure 2. Because $\rho=S(\sigma)$, and S is not in $\Gamma_T(2)$, the comparison with [18] is not immediate. The few phases appearing in their diagram do in fact have the same topology as the S-transform of figure 2, but no fixed point or RG flow structure was suggested. Also, the detailed geometry differs, presumably because of an arbitrary normalization in their approach.

It is a pleasure to thank P Aspinwall, G Ross, C Series and T Skjelbred for useful discussions. This work was supported by the Norwegian Research Council for Science and Humanities (NAVF) and the British Science and Engineering Research Council (SERC).

† Because the authors of [15] claim to have performed the experiments at $\sigma_{xy}=1/2$, there are probably significant systematic errors in addition to the 20% error bars quoted in table 1.

References

[1] Lütken C A and Ross G G 1992 *Phys. Rev.* B **45** 11837
[2] Kramers H A and Wannier G H 1941 *Phys. Rev.* **60** 252
[3] Lütken C A and Ross G G 1993 *Phys. Rev.* B **48**
[4] Rankin R A 1977 *Modular Forms and Functions* (Cambridge: Cambridge University Press)
[5] Serre J-P 1980 *Trees* (Berlin: Springer) (translated from the original French edition: 1977 *Arbres, Amalgames, SL_2* (Society of Mathematics, France, Astérisque No. 46)
[6] Cardy J L 1982 *Nucl. Phys.* B **205** 17
[7] Laughlin R 1983 *Phys. Rev. Lett.* **50** 1395
[8] Haldane F D M 1983 *Phys. Rev. Lett.* **51** 605
[9] Halperin B 1984 *Phys. Rev. Lett.* 52 1583
[10] MacDonald A H, Aers G C and Dharma-wardana M W C 1985 *Phys. Rev.* B **31** 5529
[11] Laughlin R B 1988 *Science* **242** 525
[12] Lee D-H and Fisher M P A 1990 *Phys. Rev. Lett.* **64** 1313
[13] Lütken C A 1993 *Nucl. Phys.* B **396** 670
[14] Wei H P, Tsui D C and Pruisken A M M 1985 *Phys. Rev.* B **33** 1488
[15] Mallett J R, Clark R G, Harris J J and Foxon C T 1989 *High Magnetic Fields in Semiconductor Physics II* ed G Landwehr (Berlin: Springer)
[16] Mallett J R 1989 doctoral dissertation, Oxford University (unpublished)
[17] Halperin B I, Lee P A and Read N 1993 *Phys. Rev.* B **47** 7312
[18] Kivelson S, Lee D-H and Zhang S-C 1992 *Phys. Rev.* B **46** 2223